Science
AAAS

Supplementary Materials for

Gene edited and engineered stem cell platform drives immunotherapy for brain metastatic melanomas

Nobuhiko Kanaya, Khalid Shah *et al.*

Correspondence to: Khalid Shah, MS, PhD, kshah@bwh.harvard.edu

This PDF file includes:

Supplementary Materials and Methods
figs. S1 to S9
Tables S1

Supplementary Materials and Methods

TCGA analysis: mRNA expression profile and patient information of tumor samples were extracted from the R2 Genomics Analysis Visualization Platform (https://hgserver1.amc.nl.cgi-bin/r2/main.cgi). Set-score was determined by subtracting the average z-score of negative regulating genes from the average z-score of positive regulating genes, determined by pathway analysis of GO:0014065 (http://www.informatics.jax.org/go/term/GO:0014065). The following genes were analyzed as positive regulators of the PI3K/AKT pathway: Agap2, Agt, Akt1, Angpt1, Cat, Cbl, Ccl5, Cd28, Cntf, Csf3, Dcn, Egf, Erbb4, F2, F2r, F2rl1, Fgf2, Fgr, Flt1, Fn1, Fshr, Fyn, Gper1, Hax1, Hcls1, Hcst, Hgf, Igf1r, Il18, Insr, Jak2, Kdr, Lep, Maz, Mydgf, Myoc, Nedd4, Nkx3-1, Nrg1, Ntrk1, Ntrk2, Ntrk3, Osm, Pdgfa, Pdgfb, Pdgfc, Pdgfd, Pdgfrb, Pik3ap1, Pld2, Plxnb1, Ppard, Prr5, Prr5l, Ptk2, Ptpn6, Rara, Reln, Rgl2, Ror1, Ror2, Selp, Sema4d, Serpina12, Sirt1, Sox9, Tek, Tgfb2, Ube3a, Unc5b, Vegfa, Wnt16. The negative regulators of the PI3K/AKT pathway were: Btn2a2, Cryba1, Dab2ip, Inpp5e, Klf4, Ncor1, Nlrc3, Obscn, Pik3ip1, Pten, Serpine2, Slc9a3r1, Slc9a3r2, Stambp, Tsc2, Twist1. Group determination of PTEN-expression and pathway activation was done based on median and extreme quartiles, respectively. Immune phenotyping data of TCGA patients was based on Thorsson et al study (*1*). Extracted data were entered into GraphPad Prism 9 software to generate graphs and heatmaps and do the statistical analysis.

Cell viability assay: Cells were seeded in 96-well plates (1×10^3 cells/well) (n=5) and treated with oHSV at the indicated MOI. Cell viability was determined 2-3 days after treatment by adding a Cell Titer Glo (Promega). For co-cultures of SC and melanoma cells, SCs were infected with oHSV (MOI=2, 5) for 6 hours, washed with phosphate-buffered saline (PBS) 2 times and then co-cultured with Y1.1-GFl, Y2.1-GFI and UV2-GFI cells at indicated ratio on 96-well plate ($1x10^3$ cells /well). Cell viability assay was performed by measuring the in vitro Firefly luciferase bioluminescence.

Immunofluorescence: Tissues were extracted and fixed in 4% paraformaldehyde in PBS overnight at 4°C, followed by further fixation at 4°C in 20% sucrose in PBS overnight and 30% sucrose in PBS overnight. 8-30 µm sections were cut at the halfway points of the tumor diameters. Fluorescent staining of untreated tumors and spleens was performed without antigen retrieval according to standard protocol (Cell Signaling Technology) with an additional methanol permeabilization step added after thawing sections to room temperature. Tumor sections were incubated with primary antibody against CD3, CD8, CD4, CD68 (Abcam),

CD11c (Cell Signaling Technology), IBA1 (FJIFILM) and probed with Alexa Fluor 647, or Alexa Fluor 555 conjugated secondary antibody (Abcam). The number of cells expressing CD3, CD8, CD4, CD68, CD11c and IBA1 was determined from three randomly selected fields.

Multi-cytokine and chemokine assays: SCs were treated with oHSV (0, and 2 MOI) for 24 hours, after which various cytokines and chemokines (Interleukin (IL)-1, IL-2, IL-3, IL-4, IL-5, IL-6, IL-7, IL-10, IL-12, IL-13, IL-16, IL-17, IL-23, IL-27, Chemokine (C-C motif) ligand (CCL)1, CCL2, CCL3, CCL4, CCL5, CCL11, CCL12, CCL17, C-X-C motif chemokine ligand (CXCL)1, CXCL2, CXCL9, CXCL10, CXCL11, CXCL12, CXCL13, macrophage colony-stimulating factor (M-CSF), Granulocyte Colony Stimulating Factor (G-CSF), Granulocyte Macrophage colony-stimulating Factor (GM-CSF), Soluble Intercellular Adhesion Molecule-1 (ICAM-1), interferon (IFN)-gamma, tumor necrosis factor (TNF)-alpha, Tissue inhibitors of metalloproteinase (TIMP)-1, Triggering receptor expressed on myeloid cell (TREM)-1, C5a) in the supernatants were measured using a mouse cytokine array (R&D Systems), according to the manufacturers' protocols.

ATP assays: Y1.1, Y2.1, and UV2 cells were treated with oHSV (0, 2, and 5 MOI) for 24 hours, and 48 hours (n = 5), after which concentrations of extracellular ATP in the supernatants were measured using an ENLITEN ATP assay (Promega) according to the manufacturers' protocols.

Western blot analysis: Proteins extracted from whole-cell lysates were electrophoresed on 10-20% SDS-polyacrylamide gels and transferred to PVDF membrane (Merck Millipore). The membranes were incubated with primary antibodies against GM-CSF (Abcam), HA-Tag, His-Tag, phospho-AKT, phospho-mammalian target of rapamycin (mTOR), Phosphoinositide 3-kinase (p-PI3K), Caspase-8, poly (ADP ribose) polymerase (PARP), phospho-MLKL, LC3B, β-Actin, Phosphatase and tensin homologue deleted on chromosome ten (PTEN) (Cell Signaling Technology), and Vinculin (Sigma), followed by peroxidase-linked secondary antibody. The membrane was probed with secondary antibodies and developed with ECL (Thermo Fisher Scientific). Equal loading of samples was confirmed using Vinculin, or β-Actin.

RNA-sequencing: C57BL/6 mice were intrathecally implanted with UV2-GFl (5×10^4 cells per mouse), and treated with intrathecal injection of SC based therapy on days 5. On day 12, mice were euthanized and tumors were collected. Total RNA was extracted from tumor tissues using RNeasy Mini Kit (Qiagen, 74104) following the manufacturer's protocol and kept at -80℃ until analysis. Sample quality was checked using

Agilent 2100 Bioanalyzer (Agilent). Library preparation and sequencing were performed by BGI Genomics using DNBseq platform (BGI) at a total of 4.47Gb bases per sample. After sequencing, the raw reads were filtered using Soapnuke (BGI). After getting clean reads, hierarchical indexing for spliced alignment of transcripts (HISAT2) was used to align the clean reads to the reference genome (Mus musculus, GCF_000001635.9_GRCm39) (*2*). The average mapping ratio with reference genome is 95.60%, the average mapping ratio with gene is 90.45%, and 55417 genes were identified. For differential gene expression analysis, pairwise comparisons between the RNA-seq counts between different experimental groups were performed using DESeq2 in RNAdetector (*3*). Genes with an adjusted p value less than 0.05 were considered to be differentially expressed. For gene ontology pathway enrichment analysis, differentially expressed genes between groups were analysed using ShinyGO v0.75 (*4*). Pathways with an adjusted enrichment p value less than 0.05 were considered to be significantly enriched.

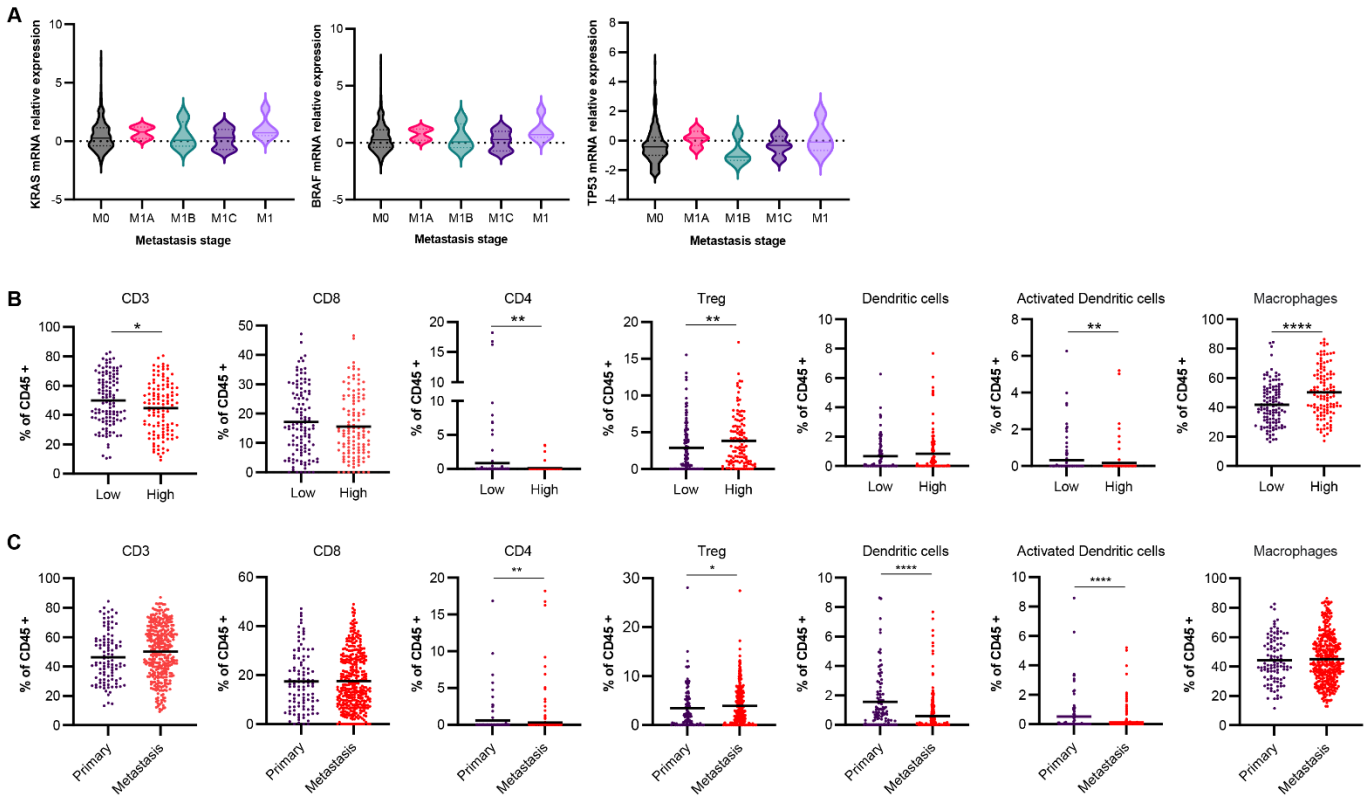

Figure. S1 PTEN deficiency is correlated with melanoma brain metastasis and immune suppression.(A) mRNA expression of BRAF, TP53 and KRAS in patient samples of different metastatic stages (M0, M1A, M1B, M1C, M1) from TCGA database (*n* = 337). (**B)** Immune profile analysis of the tumor microenvironment of melanoma patients comparing high and low PI3K/AKT pathway expression based on their set-score of 88 genes regulating the PI3K/AKT pathway. Data were derived from TCGA database. **: P<0.05. **: P<0.01, ****: P<0.0001.* (**C**) Immune profiles analysis in primary and metastatic melanoma from TCGA database. **: P<0.05. **: P<0.01, ****: P<0.0001.*

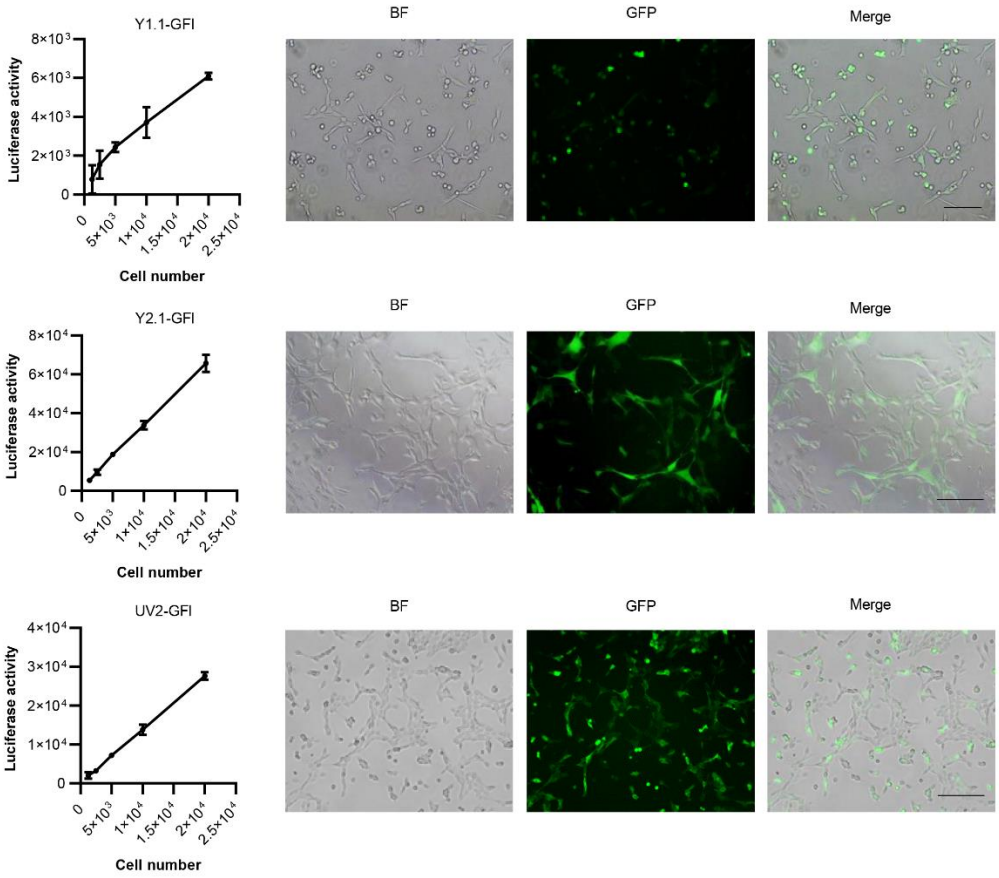

Figure. S2. Characterizing engineered murine melanoma cells. (Left) Correlation between Fluc signals in vitro and the number of cells (Y1.1-GFI, Y2.1-GFI, and UV2-GFI) engineered to express Fluc that were used in this study (*n*=5). These cells were seeded in different numbers and incubated with medium containing D-luciferin. Data are represented as mean + SD. (Right). Microscopic imaging (Brightfield (BF) and GFP) of engineered cells. Scar bar, 100 μm.

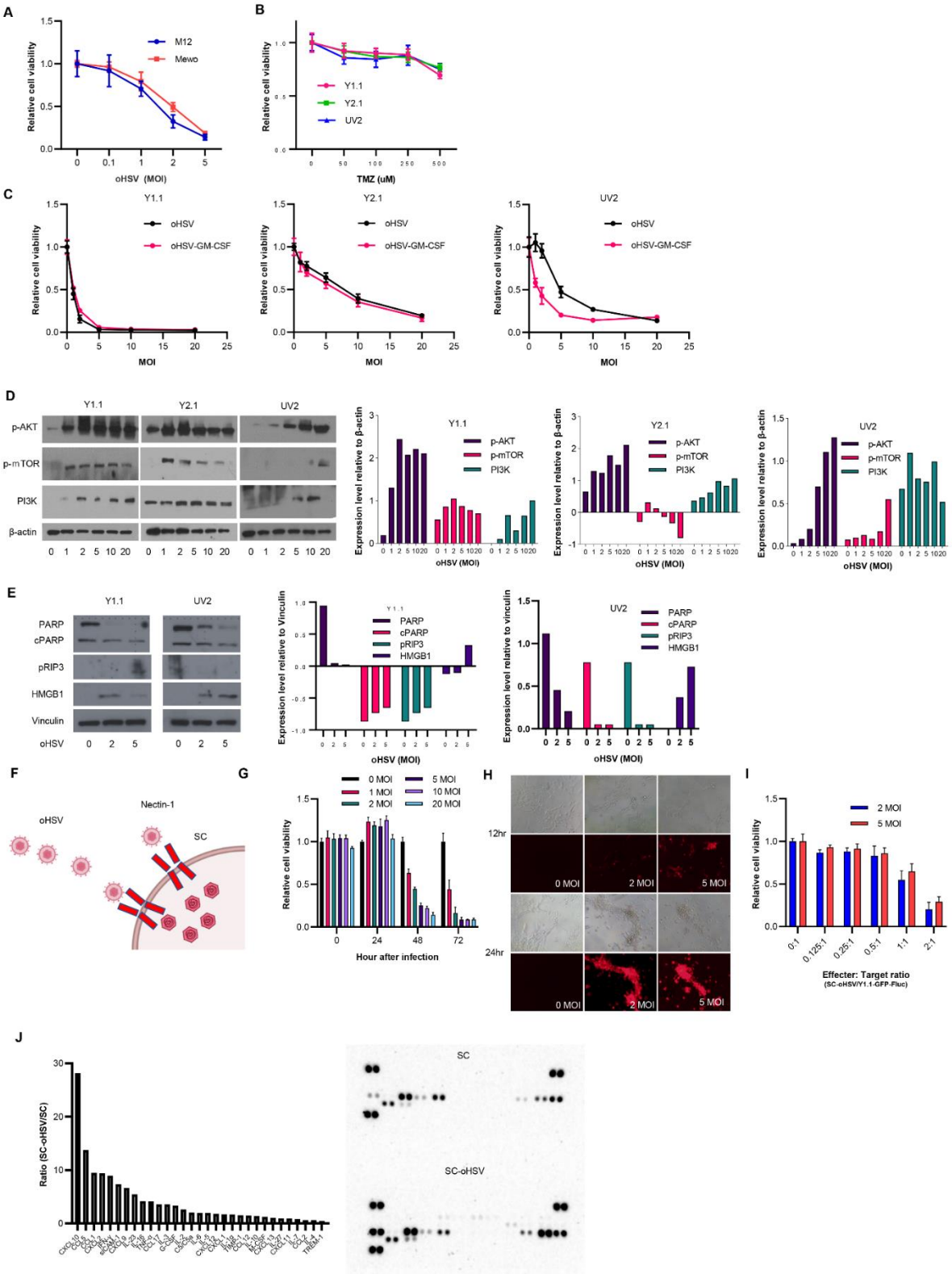

Figure. S3. Utility of SCs as carriers for oHSV. (A) Cell viability assay of human melanoma (Mewo and M12) cells was assessed 3 days after oHSV treatment at the indicated doses (MOI) (*n*=5). Data are represented as mean ± SD. **(B)** Cell viability assay of murine melanoma cells (Y1.1, Y2.1 and UV2) was assessed 3 days after Temozolomide (TMZ) at the indicated doses (*n*=5). Data are represented as mean ± SD. **(C)** Cell viability assay of melanoma cells was assessed 3 days after oHSV or oHSV-GM-CSF treatment at the indicated doses (MOI) (*n*=5). Data are represented as mean ± SD. **(D)** Left. Whole-cell lysates of Y1.1, Y2.1 and UV2 cells collected 3 days after oHSV treatment (0, 1, 2, 5, 10, and 20 MOI) were subjected to western blot analysis of p-AKT, p-mTOR, PI3K and β-actin expression. Right. Expression levels of p-AKT, p-mTOR, and PI3K relative to β-actin. **(E)** Left. Whole-cell lysates of Y1.1 and UV2 cells collected 3 days after oHSV treatment (0, 1, 2, 5, 10, and 20 MOI) were subjected to western blot analysis of PARP, pRIP3, HMGB1, and Vinculin expression. Right. Expression levels of PARP, pRIP3, and HMGB1 relative to Vinculin. **(F)** Schema showing oHSV infection of SCs via Nectin-1 receptors. **(G)** SCs were assessed using cell viability assay 0-3 days after oHSV treatment infected at the indicated doses (MOI). (*n*=5 per group). Data are represented as mean + SD. **(H)**

Representative light microscopy and fluorescence microscopy images of SCs infected with 2 and 5 MOI oHSV-FmC at 12 hours and 24 hours after infection. **(I)** Plot showing quantified differences in Y1.1-GFl cell viabilities between co-cultures with SC-oHSV at 2 and 5 MOI 72h (*n*=5 per group). Data are represented as mean + SD. **(J)** Representative plots of multi-cytokine and chemokine assays 24 hours after oHSV infection (0, 2MOI). Cytokines and chemokines secreted from SC-oHSV cells were measured using multi-cytokine and chemokine assays 24 hours after oHSV infection (0, 2MOI) and ratio of 2 to 0 MOI was plotted for each cytokine or chemokine by ImageJ. (Left): Qiatification and (Right) Blotting of multi-cytokine and chemokine assays with SC-oHSV and SC.

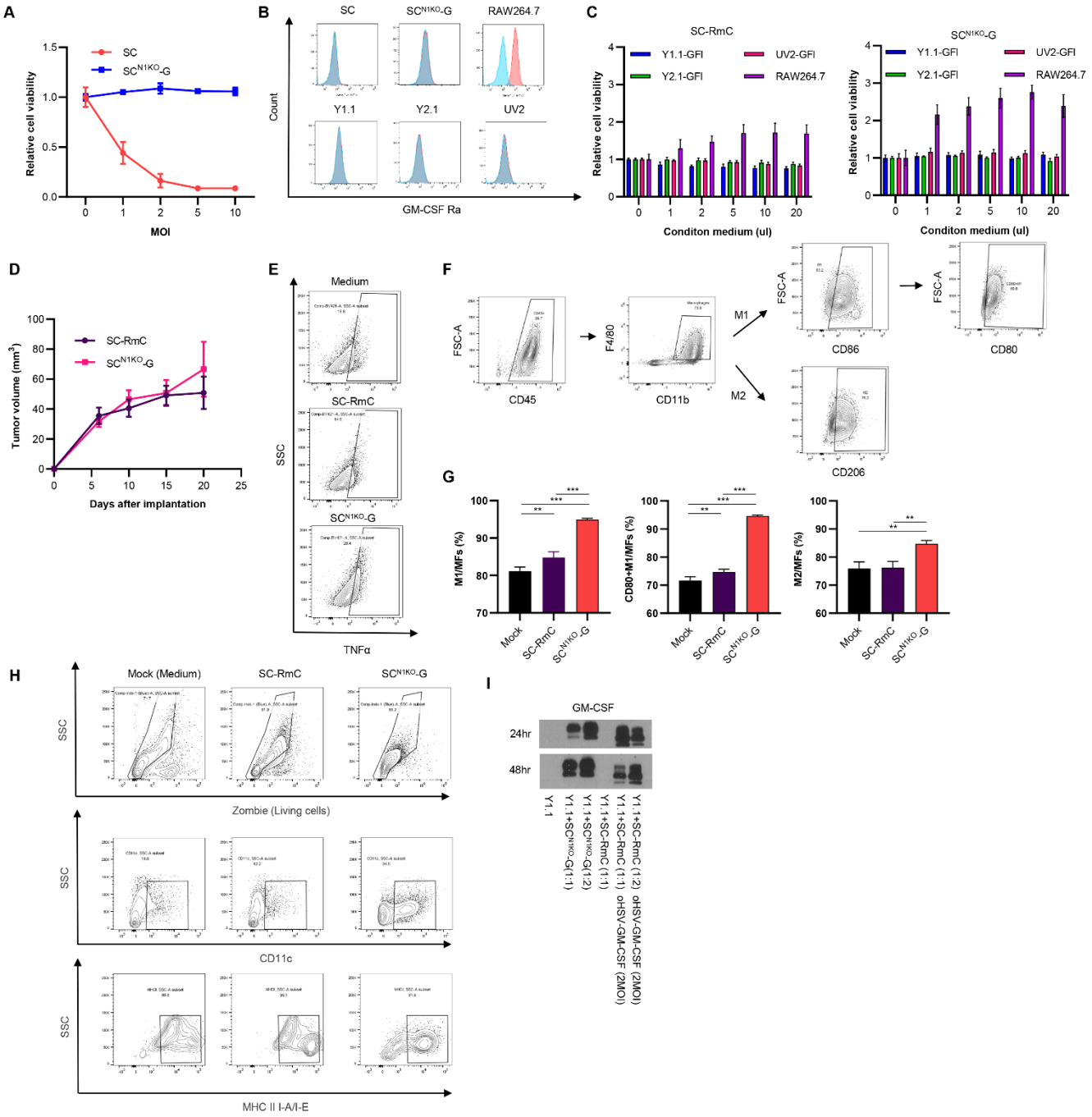

Figure. S4. Establishment of oHSV-resistant SCs secreting GM-CSF and the influence on dendritic cells and macrophages. **(A)** Cell viability assays showing SC^{N1KO}-GM-CSF (SC^{N1KO}-G) resistance to oHSV compared to SC (*n*=5 per group). Data are represented as mean ± SD. **(B)** Expression of GM-CSF Ra on SCs, RAW264.7 cells and murine melanoma cells by flowcytometry (FCM). **(C)** Cell viability assays showing influence of SC^{N1KO}-GM-CSF (SC^{N1KO}-G) and SC-Rluc-mCherry (RmC) on murine macrophage (RAW264.7) and melanoma (Y1.1-GFl, Y2.1-GFl and UV2-GFl) cell lines. (*n*=5 per group). Data are represented as mean + SD. **(D)** Plots showing subcutaneous Y1.1-GFl tumor growth in mice treated with control SC-RmC (*n* = 8) or SC^{N1KO}-G (*n* = 8). In Y1.1-GFl subcutaneous melanoma mouse model, tumor was treated with SC-RmC or SC^{N1KO}-G intratumorally twice (day7 and day11) starting 7 days after inoculation. Tumor volumes were measured every 5 days post-implantation. Data are represented as mean ± SEM. **(E)** Representative plots of TNFα positive RAW264.7 cells by FCM after incubation with SC^{N1KO}-G conditioned medium (CM) for 4 days (*n*=3 per group). **(F)** Representative plots of M1 macrophages (CD45+CD11b+F4/80+CD86+) and M2 macrophages (CD45+CD11b+F4/80+CD206+) by FCM. **: p<0.01, ***: p<0.001, ****: p<0.0001. **(G)** Shown is the effect of SC^{N1KO}-G conditioned medium (CM) on differentiation into M1 and M2 macrophages from murine bone marrow derived macrophages by FCM after incubation for 3 days (*n*=3 per group). Data are represented as mean + SD. **: P<0.05. **: P<0.01, ***: P<0.001.* **(H)** Flow cytometry plots showing the effect of SCN1KO-G conditioned medium (CM) on differentiation to dendritic cells (DCs) and mature DCs from murine bone marrow cells (CD45+ cells) by FCM after incubation for 4 days (n=3-4 per group). Representative plots of dendritic cells

(CD45+CD11b+CD11c+) and mature dendritic cells (CD45+CD11b+CD11c+MHC II I-A/I-E+) by FCM. **(I)** Western blot analysis showing GM-CSF release from in vitro co-culture with Y1.1-GFl cells and SC^{N1KO}-G or SC-RmC and oHSV-GM-CSF.

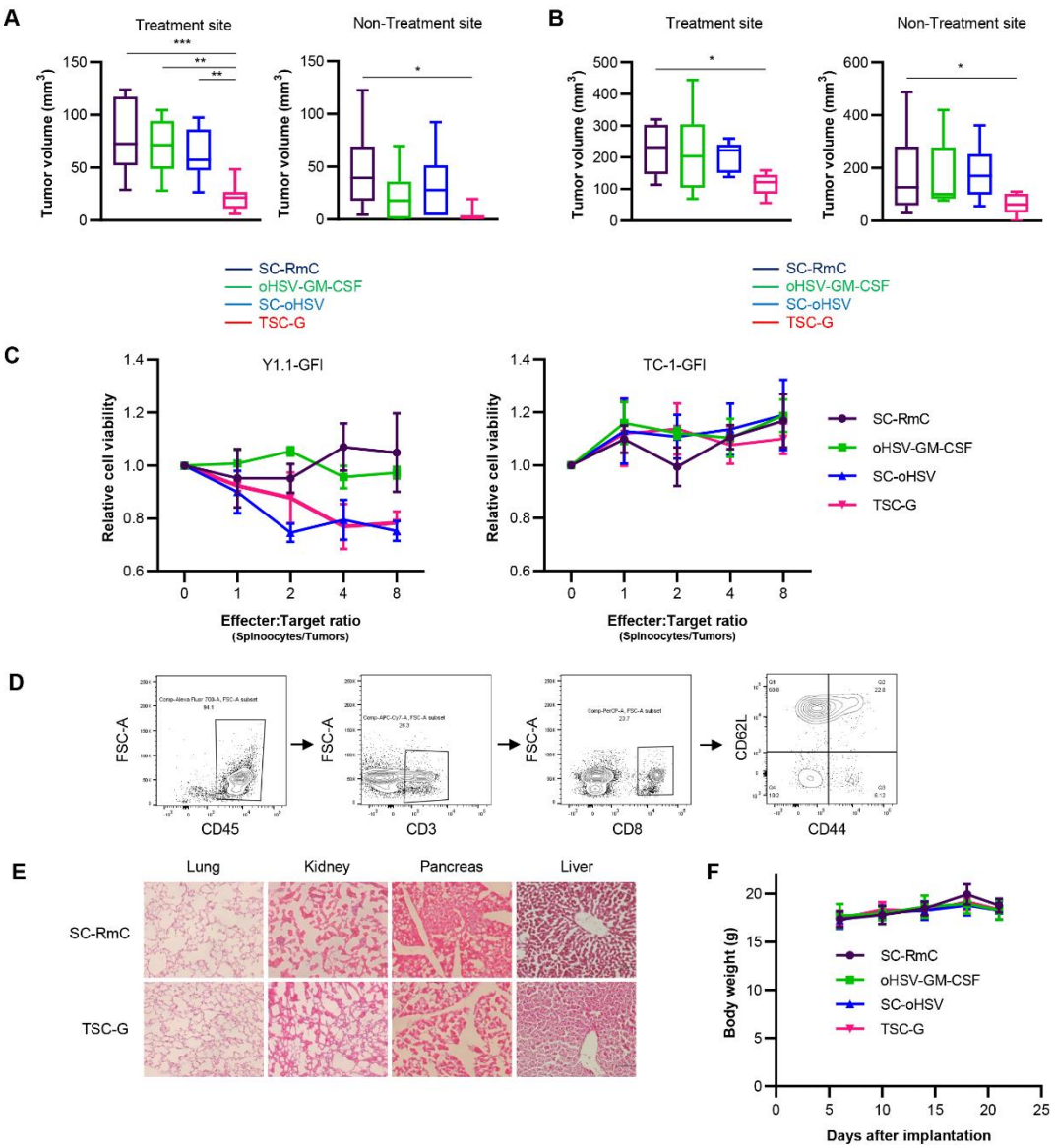

Figure. S5. TSC-G therapy generates systemic immunity against bilateral flank PTEN deficient melanomas in vivo. (A) Tumor volume (mm^3) at day 20 after treatment with control SC-Rluc-mCherry (RmC) (*n*=7), oHSV-GM-CSF (*n*=7), SC-oHSV (*n*=8), or TSC-G (*n*=8). (Left) in Y1.1-GFl bilateral flank model and **(B)** at day 18 after treatment with control SC-RmC (*n*=7), oHSV-GM-CSF (*n*=7), SC-oHSV (*n*=8), or TSC-G (*n*=8) in bilateral UV2-GFl subcutaneous model. Data are represented as mean ± SEM. **: P<0.05. **: P<0.01, ***: P<0.001.* **(C)** Splenocytes from mice after treatment (*n*=3 per group) in bilateral Y1.1-GFl subcutaneous tumor model were incubated at 37°C with Y1.1-GFl melanoma cells (left) or TC-1-GFl lung cancer cells (right) at increasing effector cell: target cell ratios (1:1-8:1). Data are represented as mean ± SD. **(D)** Representative plots of central memory and effecter memory CD8+ cells on splenocytes at 30 days after treatment in bilateral UV2-GFl subcutaneous model. **(E)** H&E staining to assess toxicity in major organs after treatment. Scale bar 100 μm. **(F)** Variation in body weights of mice after TSC-G, oHSV-GM-CSF and SC-oHSV treatment in Y1.1-GFl bilateral flank model. Data are represented as mean ± SD.

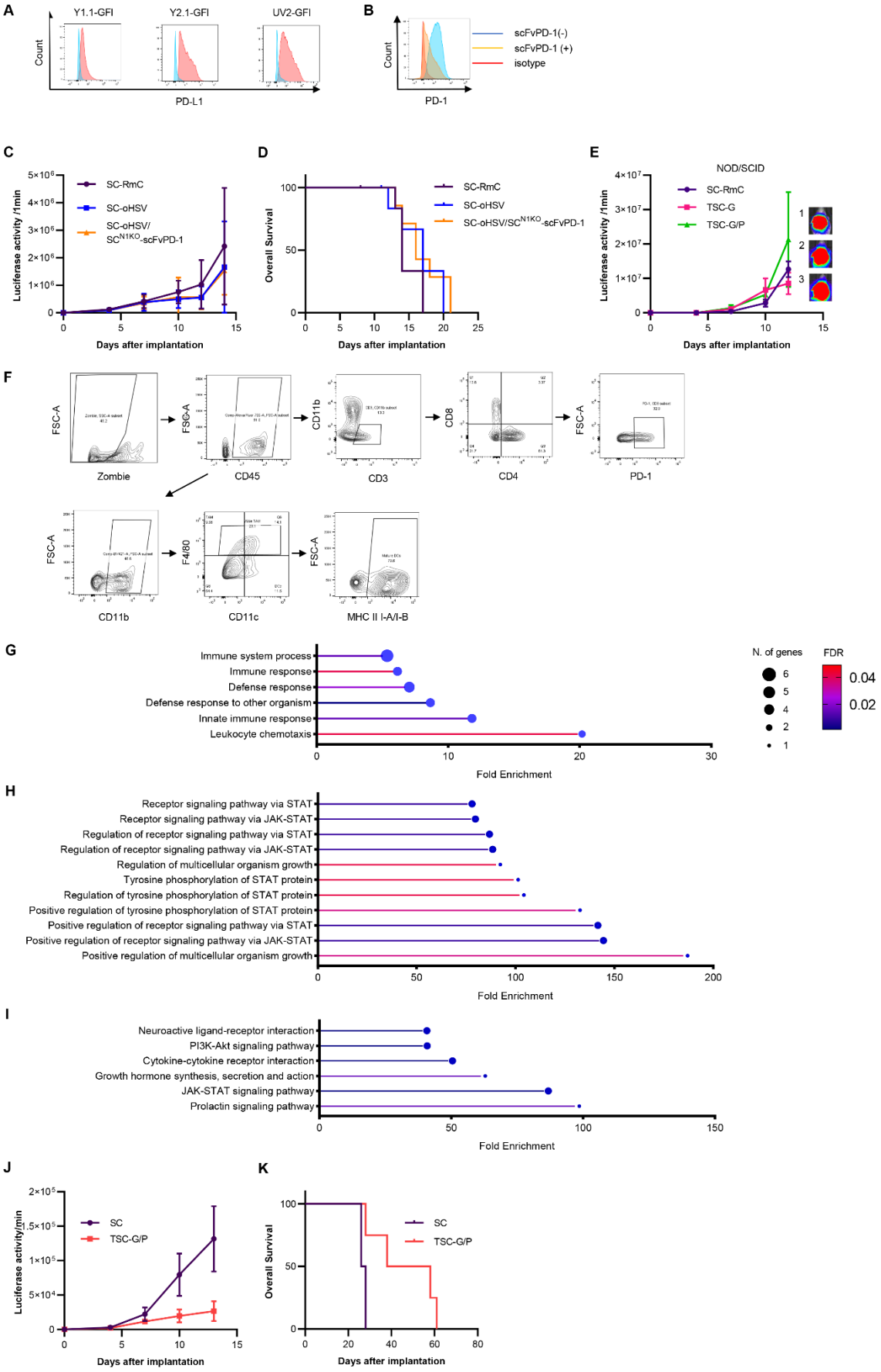

Figure. S6. SCs secreting dual immunomodulators with SC-oHSV (TSC) to treat immunosuppressive leptomeningeal metastasis. (A) Flowcytometry (FCM) showing PD-L1 expression on murine melanoma cells in vitro. **(B)** FCM showing PD-1 expression on C57BL6 derived CD3+spenocytes 48 hours after incubation with condition medium of SC^{N1KO}-scFvPD-1 in ex vivo. **(C)** Fluc signal curves and representative BLI images of mice bearing UV2-GFl tumors treated with SC-RmC (*n*=6), SC-oHSV (*n*=6) or SC-oHSV+SC^{N1KO}-scFvPD-1 (*n*=6). Data are represented as mean ± SEM. **(D)** Kaplan-Meier curves of overall survival of mice

from tumor implantation. **(E)** Fluc signal curves and representative BLI images of UV2-GFI bearing NOD/SCID mice after treatment with SC-RmC (*n*=4), TSC-G (*n*=4), or TSC-G/P (*n*=4). Data are represented as mean ± SEM. **(F)** Representative plots of gating for immune profiling of Fig. 5I. **(G)** GO analysis of immune associated pathways (Upregulated genes) after the treatment (TSC-G or TSC-G/P versus SC-RmC). **(H)** GO analysis of JAK-STAT pathways (Downregulated genes) after the treatment (TSC-G or TSC-G/P versus SC-RmC). **(I)** KEGG analysis of PI3K-AKT and JAK-STAT pathways (Downregulated genes) after the treatment (TSC-G or TSC-G/P versus SC-RmC). **(J)** SCs were intrathecally (IT) administrated one time 5 days after implantation of tumors in the Y2.1-GFl LM mouse model. Tumor volumes were measured every 3-4 days by BLI imaging. Fluc signal curves and representative BLI images of mice bearing Y2.1-GFl tumors treated with SC-RmC (*n*=4) or TSC-G or TSC-G/P (*n*=4). Data are represented as mean ± SEM. **(K)** Kaplan-Meier curves of overall survival of mice bearing Y2.1-GFI tumors. **: P<0.05.*

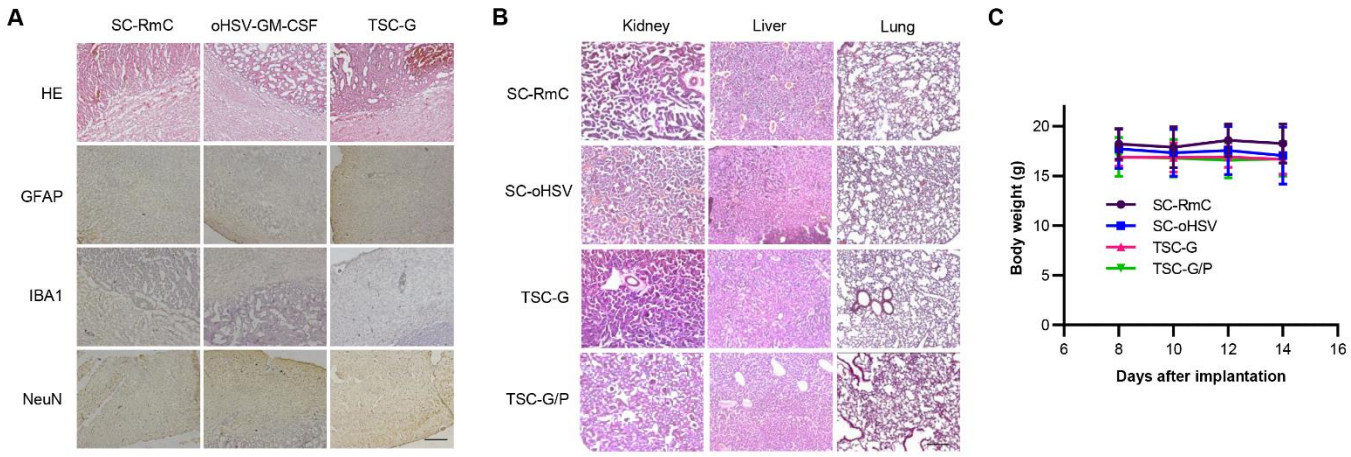

Figure. S7. Safety of SCs secreting dual immunomodulators with SC-oHSV (TSC) in metastatic melanoma mouse model. **(A)** Representative photomicrographs of Hematoxylin and eosin (H&E) stain and immunohistochemistry of NeuN, GFAP and IBA1 in brain from intracranially injected UV2-GFl-bearing mice treated with SC-RmC, oHSV-GM-CSF and TSC-G (*n*=3, Scale bars, 100 μm). **(B)** H&E staining showing changes in major organs after treatment of TSC-G or TSC-G/P to assess toxicity. Scale bar 100 μm. **(C)** Change in body weights of mice after intrathecal injection of TSC-G or TSC-G/P. Data are represented as mean ± SD.

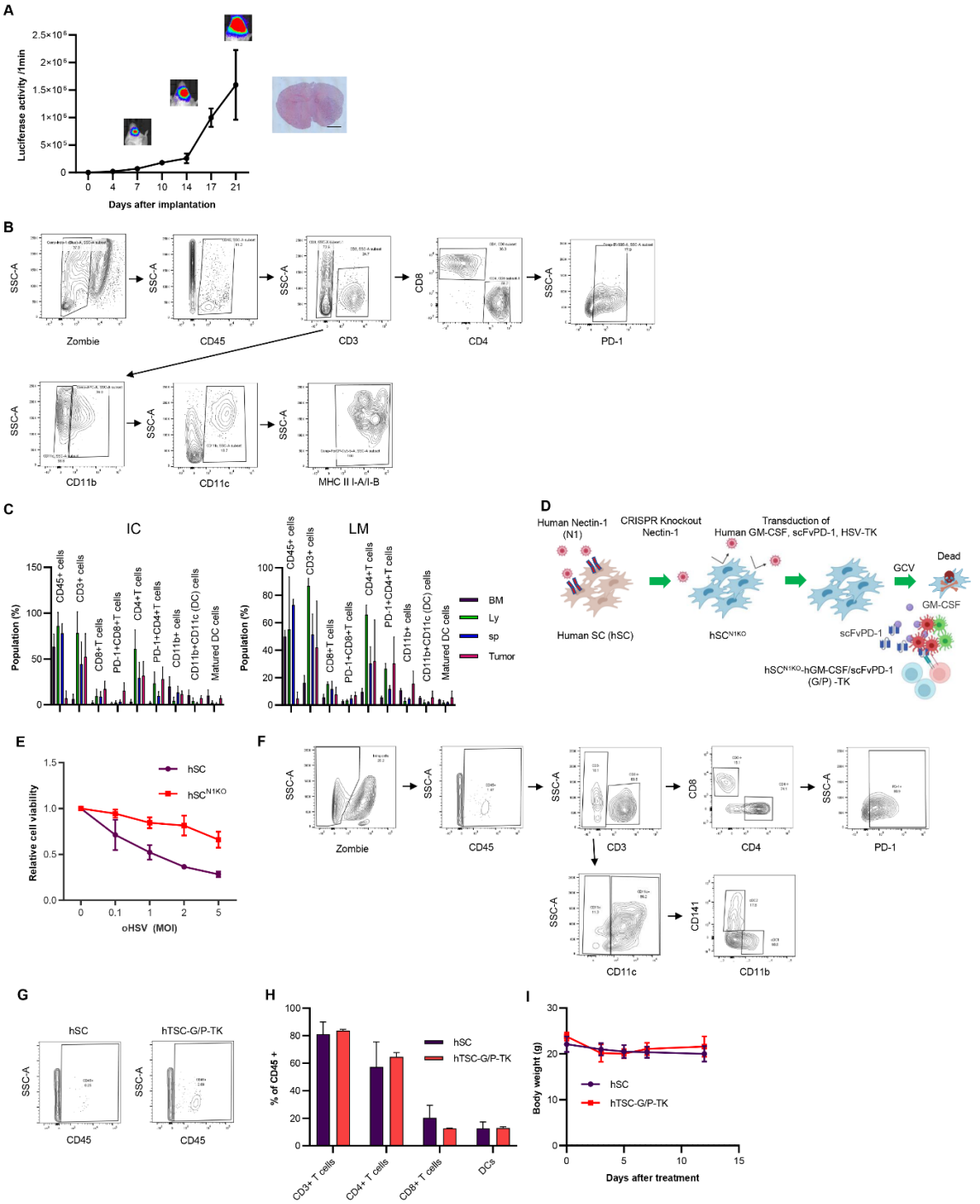

Figure. S8. Establishment of patient derived PTEN deficient melanoma brain metastasis BLT mouse model, and allogeneic SCs releasing human GM-CSF/scFvPD-1-TK and SC-oHSV (hTSC-G/P-TK) to treat brain metastasis.

(A) BLI signal curve of intracranially injected M12-GFl-bearing NOD/SCID mice (*n*=5). Data are represented as mean ± SEM. **(B)** Representative plots of immune profiling in UV2-GFl brain tumor BLT mouse model and leptomeningeal metastasis BLT mouse model. **(C)** Flowcytometric (FCM) analysis of immune profiling of brain M12-GFl tumor model (IC) and leptomeningeal metastasis model (LM) at the bone marrow cells (BM), the splenocytes (Sp) and the cervical lymph node (Ly) (*n*=4). Data are represented as mean + SD. **(D)** Scheme showing creation of human SC^{N1KO} (hSC^{N1KO}) -human GM-CSF/scFvPD-1 (G/P)-TK. To establish oHSV-resistant hSC-G/P-TK, human Necin-1 on SCs was knocked out by CRISPR/Cas9 gene editing and hSC^{N1KO} were transduced with LVs bearing GM-CSF and scFvPD-1 and also HSV-TK as a safety switch. **(E)** Cell viability assays showing human SC^{N1KO} resistance to oHSV compared to human SC in vitro (*n*=5). Data are represented as mean ± SD. **(F)** Representative plots of gating for immune profiling 10 days after treatment by FCM (*n*=3 per group). **(G)** Representative plots of gating for CD45+ cells 10 days after treatment by FCM. **(H)** FCM analysis of immune cells (CD45+) collected from M12-GFl leptomeningeal metastases10 days after treatment (*n*=3 per group). Data are represented as mean + SD. **(I)** Variation in body weights of mice after treatment in patient derived melanoma LM BLT mouse model (each group: *n*=4). Data are represented as mean ± SD.

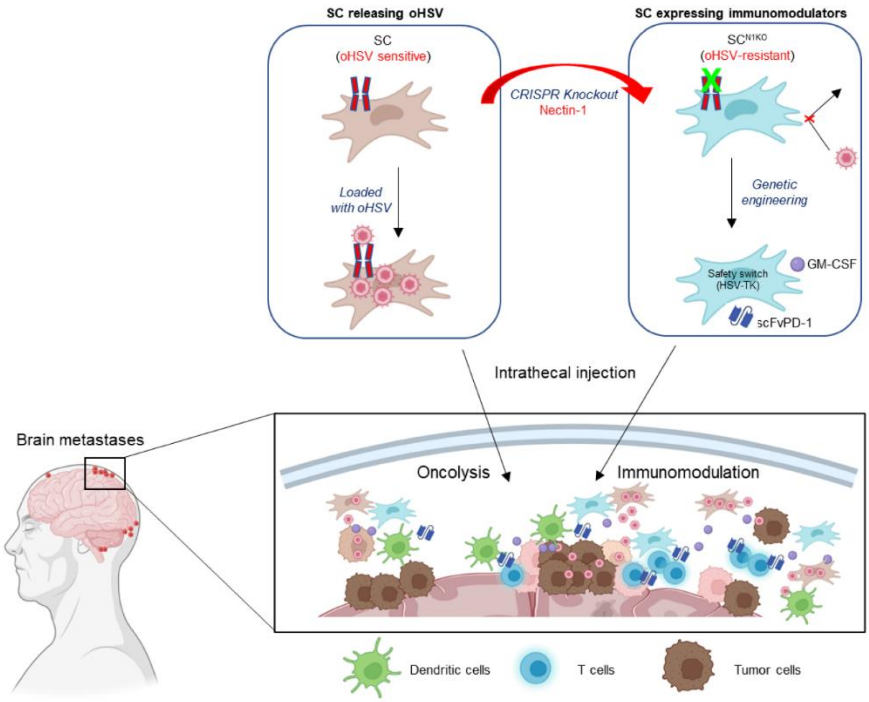

Figure. S9. Concept of stem cells (SCs) based therapy with oHSV and immunomodulators in melanoma leptomeningeal metastasis. TSC-G/P effectively suppressed immunosuppressive PTEN deficient leptomeningeal metastasis in both syngeneic and patient derived-humanized mouse models by the enhance of antitumor immunity through activation of dendritic cells and T cells.